Coventry University

Coventry University Repository for the Virtual Environment (CURVE)

Author name: Saidani, M.
Title: Behaviour of welded T-end connection to rectangular hollow section (RHS) in axial tension.
Article & version: Post-print version
Original citation & hyperlink:
Saidani, M. (2008) Behaviour of welded T-end connection to rectangular hollow section (RHS) in axial tension. *Journal of Constructional Steel Research*, volume 64 (4): 447-453.
http://dx.doi.org/10.1016/j.jcsr.2007.10.003

Copyright © and Moral Rights are retained by the author(s) and/ or other copyright owners. A copy can be downloaded for personal non-commercial research or study, without prior permission or charge. This item cannot be reproduced or quoted extensively from without first obtaining permission in writing from the copyright holder(s). The content must not be changed in any way or sold commercially in any format or medium without the formal permission of the copyright holders.

This document is the author's final manuscript version of the journal article, incorporating any revisions agreed during the peer-review process. Some differences between the published version and this version may remain and you are advised to consult the published version if you wish to cite from it.

Available in the CURVE Research Collection: October 2012

http://curve.coventry.ac.uk/open

Behaviour of welded T-end connection to Rectangular Hollow Section (RHS) in axial tension

M. Saidani[a]

Faculty of Engineering and Computing, Civil Engineering, Coventry University, Priory Street, Coventry CV1 5FB, England, UK

Abstract

This paper presents the results of an experimental investigation into the behaviour of welded T-end connections to rectangular hollow section (RHS) members subjected to axial tension. A total of 19 specimens were tested to failure. Parameters considered for the investigation were the tube size and the cap plate thickness. The cleat plate thickness was kept constant for all tests. The cleat plate orientation relative to the tube was investigated and was found to affect the joint strength. There was evidence of shear lag taking place. The test results also revealed that the use of very thick cap plates (more than 20 mm) does not lead to increased joint capacity. The yield line analysis was used to predict the failure loads and comparison is made with the test results.

Keywords: Connection; hollow section; cap plate; strength; modes of failure.

1. Introduction

Structural Steel Hollow Section (SSHS) members are known to possess many advantages over equivalent open sections, including better resistance to torsion as well as tension and compression loading, aesthetic appearance and economy in terms of

[a] Correspondence e-mail address: m.saidani@coventry .ac.uk // Telephone/Fax: 00 44 (0)24768883485

material cost [1]. Connections between SSHS members could be made simple by cutting the ends and welding together. However, depending on joint configuration and number of members connected, this may result in complex and expensive connections. The alternative would be to connect the members together through some other means. Fig. 1 shows types of end connection details for hollow tubes that are used in practice. One of the most economic solutions is to weld a cap plate to the tube and then weld on to it a cleat plate (Fig. 2). The connection could be made entirely in the workshop, thus reducing labour work on site and cost.

In the UK there is very little guidance on the design of welded T-end connections. Elsewhere, research work was mainly carried out by Kitipornchai and Traves [2], Stevens and Kitipornchai [3], and Granstrom [4]. Syam and Chapman [5] attempted to develop design models for T-end connection, as well as for other types of structural steel hollow section connections. Packer and Henderson [6] produced a design guide in which design guidelines are given for T-end connection to a tube and gusset plate.

The absence of design recommendations very often leads designers to specify uneconomical solutions. Research has shown that welded T-end connections subjected to uniform tension may fail in different ways [2]. The failure mode is dictated by parameters such as tube wall thickness, cap plate thickness, cleat plate thickness, and weld quality and size.

The possible resulting modes of failure are: (i) Tube yielding; (ii) Local fracture in tube (in the region adjacent to weld); (iii) Fracture of the weld; (iv) Yielding of the cap plate; (v) Shear failure of the cap plate; (vi) Yielding of the cleat plate. A combination of more than one mode of failure is also possible. In a truss environment, commonly in lateral wind bracing members of steel frames, when the connection forms part of the

truss assembly and where the cleat plate is bolted to a gusset plate, other modes of failure are also possible.

2. Specimen properties and experimental programme

The testing programme included 19 specimens with varying tube wall and cap plate thickness. A universal testing machine with a capacity of 500kN was calibrated by independent licensed consultants external, and was used for the testing of the connections. A tensile load was applied in increments of 10kN up to failure. Strains and deformations were recorded for each load increment (Fig. 3).

Four RHS tube sizes of nominal dimensions 60x60x4.0; 80x80x4.0; 60x40x4.0; and 80x40x4.0 were chosen for the test series. Tubes of one size were cut from the same stock length, each 500 mm long. All tubes used for making the specimens were of hot-finished steel Grade S355J2H to BS EN10210-1 [7] specification. The plates used for the end and cap plates were of steel Grade S355JR to specification BS EN10025-1 [8]. Tensile testing on samples of the material used in the experimental work was carried out in order to determine Young's modulus, E, the yield and ultimate stress values. The tensile test involved straining a test sample to fracture in order to determine its mechanical properties. Test pieces were obtained by machining samples from an off-cut taken from the same batch of steel used to make the specimen. The samples were tested in accordance with BS EN 10002-1 [9]. The quality and type of weld used received a lot of attention in the preparation of the specimens. All welds were fillet weld with a throat thickness of 10 mm, and were carried out externally by a certified welder to BS EN ISO 15614-1 [10].

The specimens were loaded in axial tension, taking all necessary precautions to avoid accidental eccentricity, with strain and deformation measurements being recorded. The programme of the tested specimens is summarised in Table 1 (read in conjunction with Fig. 2 above). The values shown in Table 1 are measured values. In order to keep the investigation manageable, one cleat plate thickness was used and kept equal at t_p = 15 mm for all specimens. The length of the cleat plate was also kept constant at L_p = 150 mm for all specimens.

For specimens with a 'true' rectangular cross section, i.e. not square (specimens 12, 13, 14, 15, 16, 17, 18, and 19), two arrangements of the cleat plate were adopted. For specimens 12, 13, 14, and 15, the cleat plate was placed parallel to the longer side of the tube. However, for specimens 16, 17, 18 and 19, the cleat plate was placed parallel to the shorter side of the tube. See Table 1 below.

The test programme was devised to concentrate on the yielding of the tube wall and the deformation of the cap plate as these were found to be the main causes of failure [3]. Strain gauges (SG's) were located on the tube wall (four faces), the cap plate, and the cleat plate with the aim of closely monitoring strain (and stress) variations across the specimen. LVDT's were used to give readings of the deformations and monitor in-plane and out-of-plane movements. LVDT 2, 3, 4, and 5 were taking axial displacement readings of the tube through steel brackets that were glued onto the tube and cap plate as shown in Fig. 4. LVDT 1 was placed at the movable bottom base of the testing machine.

The strain gauges were kept far enough from welds in order to avoid any influence from the residual stresses on the readings. The total length of the tube is sufficiently long (500 mm in this case), again for the same reason. Strain gauges were placed on opposite sides so that in-plane and out-of-plane bending moments could be monitored

and calculated. In total 12 stain gauges and 5 LVDT devices were used to monitor the joint behaviour and obtain the necessary information. The LVDT devices used for testing were calibrated using slip gauges.

3. Experimental results and discussion

Examination of output from the LVDT's and SG's placed on the sides of the tube to monitor in-plane and out-of-plane displacements, revealed that these were negligible and could therefore be ignored. This confirms that precautions taken in setting up the specimens in the testing machine were adequate in limiting in-plane and out-of-plane bending stresses interfere with axial stresses from the tensile loading.

Table 2 summarises the experimental failure load (P_{UE}) results from the specimens testing. The calculated yield strength of the tube (P_Y) using measured values of the specimens is also shown in the Table. For ease of comparison, the ratio of P_{UE} / P_Y is given.

For the first specimen (No.1), the failure was due to weld fracture (see Fig. 5). On close examination of the specimen it was discovered that weld penetration was not adequate, and hence this specimen was removed from further consideration. In the subsequent specimens, failure was mainly due to tube yielding (a typical example is shown in Fig. 6), and the test was stopped after the specimen ceased take any further loading.

In Figs. 7 and 8 are shown typical load-deformation and load-strain curves for specimen No.8. The other specimens (not shown here) exhibited a similar behaviour (linear and thereafter non-linear before reaching failure). The test was stopped when the

machine stopped taking and more loading, which explains why the graph in Fig. 7 does no show the complete port-ultimate behaviour.

Investigation of the strain (stress) distribution diagrams as well the load deflection graphs revealed how difficult it was to determine the first yield point (first yield). The results also showed that stress distribution in the tube was not uniform, with high stress concentrations at the vicinity of the weld and in and around the plates.

Three particular modes of failure were observed: (a) weld fracture; (b) tube yield failure (this was when the specimen ceased taking any more load); (c) local fracture of the tube wall at the vicinity of the weld (see Table 2). Failure mode (a) would only occur if the welds were the weakest part of the connection. This was avoided in subsequent tests by better quality control of the weld. Failure mode (b) is the more general one, consisting of tube yielding (when the specimen ceased to take any more load without any visible facture anywhere). If the welds in the cap plate-tube connection and the cleat plate-tube connection are strong, then failure mode (c) may take place especially for connections with thinner plates.

As can be seen from Fig. 7, the axial deformation remained linear for load of up to 230kN (estimated first yield point). In this case, the failure load was 310kN, which gives a ratio of ultimate strength to first yield stress of 1.35. The average strains on opposite sides at mid-height of the tube (Fig. 8) were linear up to about 120kN and thereafter non-linear. It is also evident from Fig. 8, that extensive strain (stress) redistribution and strain hardening were taking place. This was also evident in the other specimens.

In order to see the effect of the orientation of the cleat plate relative to the tube, two different series of tests were conducted for tubes with a ‘true’ rectangular hollow

section (i.e. not square). In specimens 12, 13, 14, and 15 the cleat plate was placed parallel to the longer side of the tube. However, in specimens 16, 17, 18, and 19, the cleat plate was placed parallel to the shorter side of the tube (see Table 1). It is clear from the results that, overall, placing the cleat plate parallel to the longer side of the tube resulted in stronger joints than when the cleat plate is placed parallel to the shorter side of the tube. This is believed to be related to shear lag effects taking place between the welded cleat plate and the cap plate, in turn welded to the tube. Shear lag is known to occur in welded elements and has been described by Dowswell and Barber [11], and also Abi-Saad and Bauer [12]. Micro-cracks in the welds could cause shear lag effects to develop and these will have an impact on the failure load. A plausible explanation is, when the cleat plate is placed parallel to the shorter side of the tube, on the longer side of the tube the cleat plate will act as a concentrated tensile load causing more micro-cracks in the weld, and hence resulting in a less effective area resisting the applied load, which in turn will result is a lower failure load than if the cleat plate was placed parallel to the longer side of the tube, where stresses are more evenly distributed.

From a practical viewpoint it is suggested to always place the cleat plate parallel to the longer side of the tube in order to achieve maximum strength for the joint.

Examination of Table 2 reveals that, overall, the ultimate load increases with cap plate thickness and tube size, but then seems to reach an optimum value (for a cap plate thickness equal to 25 mm) before ceasing to increase thereafter as the cap plate becomes thicker. This surprising result could be caused by the significant heat affected zone (HAZ) softening in the tube wall due to welding, with the cap plate acting as a ‘heat sink’. This effect is more pronounced when a thick cap plate is welded to a thinner tube, as is the case here.

4. Yield line analysis predictions and comparison with the test results

The test results for failure loads of the specimens are now compared with results obtained from yield line predictions based on equations developed by Steven and Kitipornchai (1990). The equations take into account possible development of a number of modes of failure. These are: (i) tube yielding; (ii) cleat plate yielding; (iii) shear failure of cap plate; (iv) plastic hinges in cap plate and tube sides; (v) plastic hinges in cleat plate only.

(i) Tube yielding, where the failure load is given by:

$$P_1 = A_w \sigma_{yw} \cong 2t_w (B_w + D_w - 2t_w)\sigma_{yw} \quad (1)$$

Where, σ_{yw} is the yield stress of the tube and the other parameters are as defined in Fig. 2 above.

(ii) Cleat plate yielding, where the failure load is given by:

$$P_2 = A_{P.Net}\sigma_{YP} \quad (2)$$

Where, $A_{P.Net}$ and σ_{YP} are the net cross-sectional area and yield stress of cleat plate respectively.

(iii) Shear failure of cap plate, with failure load given by:

$$P_3 = b_c\, t_c\, \sigma_{yc} + 2\, w\, t_w\, \sigma_{yw} \quad (3)$$

Here, σ_{yc} is the yield stress of the cap plate.

This mode of failure is illustrated in Fig. 9, where a portion of the cap plate is sheared out by the applied tensile force accompanied by localised yielding of the tube. In equation (3) and Fig. 9 below, b_c and t_c are the width and thickness of the cap plate, and w is the yielded width portion in the tube given by: $w = t_p + 2w_p$, where, t_p is the cleat plate thickness and w_p is the weld size in cleat to cap plate.

(iv) Plastic hinges in cap plate and tube sides, with the failure load given by:

$$P_4 = \frac{2M_{pc}}{z} + \frac{2M_{pw}\, B_w}{z}\left(1 + \frac{2y}{x}\right) + 2\, t_w\, \sigma_{yw}\left(\lambda x + w + z\, f(\lambda)\right) \qquad (4)$$

This type of mechanisms, illustrated in Fig. 10, involves the formation of plastic hinges in the cap plate and tube sides, as well as local yielding of the tube walls. In equation (4):

$$f(\lambda) = \frac{1}{2}\left[1 + \sqrt{1+\lambda^2} + \lambda^2\, \mathrm{Ln}\left[\frac{1}{\lambda}\left(1 + \sqrt{1+\lambda^2}\right)\right]\right] \quad \text{where:}$$

M_{pc} : Plastic moment capacity of effective cap plate cross-section = $\sigma_{yc} b_c t_c^2 /4$

M_{pw} : Plastic moment capacity per unit length of tube side = $\sigma_{yw} t_w^2 /4$

B_w : Outside dimension of the tube measured parallel to cleat plate.

λ : Ratio y to z (indicating amount of shearing that occurs in the tube sidewalls).

w, x, z : Dimensions used in defining the geometry of the mechanism (Fig. 10).

$y = t_c /2$ + weld size 'w_c'

(w_c is the size of the weld between the cap plate and the tube)

$z = (D_w - t_w - w)/2$ ('w' as defined in (iii) above)

By minimising the ultimate load P_4 with respect to the distance x, distance x is found to be equal to:

$$x = \left(\frac{2M_{pw} B_w}{t_w \sigma_{yw}} \right)^{1/2}$$

(v) Plastic hinges in cap plate only, with failure load:

$$P_5 = \frac{4M_{pc}}{z} + 2t_w \sigma_{yw}(w + z) \qquad (5)$$

This mode of failure is similar to mode of failure (iv) (see above), except that both pairs of hinges form in the cap plate, rather than one pair occurring in the tube sides (Fig. 11). This failure mechanism will only control in large size tubes. All parameters in equation (5) are as defined before.

The theoretical (predicted) ultimate capacity of the connection is the smallest value obtained from all five mechanisms, i.e.: $P_{UT} = \min(P_1, P_2, P_3, P_4, P_5)$

Not all mechanism described herein have been observed in the tested specimens, as can be seen from Table 2. Nevertheless, a simple spreadsheet program was written where all parameters defined in equations (1) to (5) were computed for each of the tested specimens, using measured values. These were then used to calculate P_1 to P_5, and hence the predicted ultimate failure load, P_{UT}. The results, using specimen measured values, are shown in Table 3. The experimental failure load for each specimen is compared with the ultimate load, P_{UT}, as predicted by the yield line theory.

5. Discussion of the results

Values shown in Table 3 for P_{UT}, represent the minimum value obtained from the five yield mechanisms, using measured values. In computing the values of P_{UT} it was found that the governing mode of failure that gave the best prediction of the actual test

failure load was mode (i), i.e. P_1, as may be seen from the table, corresponding to tube yielding. This agrees with the experimental observation that in almost all specimens, except one, the governing mode of failure was that of tube yielding. Overall, agreement between test results and predicted results from the yield line mechanism agree well. However, as seen from Table 3 above, not all predictions by the yield line method are on the safe side, especially for specimens with thinner cap plate (less than or equal to 15 mm). There are a number of reasons for the discrepancy: (i) experimental errors; (ii) effect of residual stresses; (iii) shear lag effects as previously explained; (iv) yield line mechanisms not accurate enough to include the above parameters. These factors may impact on the calculated failure load values and their relative magnitude in comparison with the experimental ones, with the effect more pronounced for specimen with thinner cap plates (≤ 15mm).

A careful reading of the P_{UE}/P_{UT} values (test strength to yield line method strength) shows that for those specimens with a larger tube size (80mm), the values are low (mean value 0.80), whereas for those specimens where the tube size is smaller (60mm), the ratios are higher (mean value of 0.99), this is at the exception of specimen 1 where failure was premature due to weld fracture. This seems to suggest that there is a tube size effect, which is seen to be, overall, even more significant for specimens with thicker cap plates. A possible explanation is that this is the result of the shear lag effect not specifically investigated in this research. Work previously undertaken by Abi-Saad and Bauer [12] highlighted the impact shear lag has on the failure load in welded connections depending on tube size. Indeed, a larger tube means a more pronounced shear lag effect and a reduction in the failure load. It is worth noting that the yield

models presented here do not take into account the shear lag effect, and hence future work will need to focus on refining these accordingly.

The yield line predictions agree with the experimental observations that, overall, the connection capacity increases with cap plate thickness and tube size, but then seems to cease increasing. Again, as mentioned before, within experimental errors and owing to the fact that the yield line mechanisms do include aspects such residual stresses and shear lag effects, it is therefore hard to make a definite assessment and conclusions based on currently available information, especially that the phenomena of shear lag is still receiving a lot of attention by researchers as already mentioned.

6. Conclusions

The behaviour of welded T-end plate connections loaded in tension has been investigated through a series of tests. It was found that, apart from any weld defects (specimen No.1), the overall mode of failure of the joint is by tube yielding (when connection ceased to take any additional loading) or local fracture of the tube wall.

The findings relating to the ratio of the test strength to yield line strength seem to suggest that there is a tube size effect, leading to lower values for specimens with the larger tube size. A possible explanation is that this is the result of the shear lag effects not specifically investigated in this research and ignored by the proposed yield line models, but highlighted by other researchers.

It was found that as the cap plate gets thicker (greater than 25 mm), the capacity of the joint is seen to cease increasing, suggesting that joints with excessively thicker plates are weaker than would normally be expected and that thicker cap plates do not necessarily lead to stronger connections. This result could be explained by the HAZ

softening in the RHS tube resulting from welding, as a thick and rigid cap plate is welded to a much thinner tube.

The results also suggest that considerable stress re-distribution and strain hardening were taking place after the first yield. The effect of changing the orientation of the cap plate in relation to the tube was seen to be an important factor. This is attributed to shear lag effects occurring in welded elements, and the fact that, as already explained, when the cleat is placed parallel to the shorter side of the tube, on the longer side of the tube the cleat plate will act as a concentrated tensile load causing more micro-cracks in the weld, and hence resulting in a less effective area resisting the applied load.

Comparison of failure load of specimens from the test results with those obtained using the yield line analysis mechanisms was found not to always lead to good a agreement between the two and that the predicted failure load is not always on the safe side. As indicated in the previous section, there are a number of possible reasons for the discrepancy. Therefore, the advice to designers is that the yield line equations may not be safe to use for those specimen with thinner cap plate (≤ 15mm), and will need further refinement to include effects such as shear lag.

For specimens with true RHS (i.e. not square) tube, the designers of such connections are advised that in order to achieve higher joint capacity, it is suggested to place the cleat plate parallel to the longer side of the joint.

Acknowledgements

The author is very grateful for the generous financial and technical support received from Corus, pipes and tubes (Corby, UK), especially to Msrs E. Hole and N. Yeomans.

References

[1] Comite' International pour le Developpement et l'Etude de la Construction Tubulaire (CIDECT) British Steel and the Commission of the European Communities. *Construction with hollow sections*. Corby Northants, UK, 1984.

[2] Kitipornchai S, Traves WH. Welded T-end connections for circular hollow tubes. *Journal of Structural Engineering, American Society of Civil Engineers*, 1989, 115:12, pp. 3155-3170.

[3] Stevens N, Kitipornchai S. Limit analysis of welded tee end connections for hollow tubes. *Journal of Structural Engineering, American Society of Civil Engineers*, 1990, 116:9, pp. 2309-2323.

[4] Granstrom A. End-plate connections for rectangular hollow sections. *The Swedish Steel Construction Institute*, 1979, Report 15:15.

[5] Syam AA, Chapman BG. Design of structural steel hollow sections. Volume 1: Design Models, Australian Institute of Steel Construction, Sydney, Australia, 1996.

[6] Packer JA, Henderson JE. Hollow structural section connections and trusses: a design guide. 2nd Edition, *Canadian Institute of Steel Construction*. Toronto, Canada, 1997.

[7] BS EN 10210-1 Hot finished structural hollow sections of non-alloy and fine grain structural steels. Technical delivery requirements. British Standards Institution. UK, 1994.

[8] BS EN 10025-1 Hot rolled products of non-alloy structural steels. General delivery conditions. British Standards Institution. UK, 1994.

[9] BS EN 10002-1 Tensile testing of metallic materials. Method of test at ambient temperature. British Standards Institution. UK, 1994.

[10] BS EN ISO 15614-1 Specification and qualification of welding procedures for metallic materials. British Standards Institution. UK, 1994.

[11] Dowswell B, Barber S. Shear Lag in Rectangular Hollow Structural Sections Tension Members: Comparison of Design Equations to Test Data. Practical Periodical on Structural Design and Construction, 2005, Volume 10, Issue 3, pp. 195-199.

[12] Abi-Saad G, Bauer D. Analytical approach for shear lag in welded tension members. Canadian Journal of Civil Engineering, 2006, Volume 33, Number 4, pp. 384-394(11).

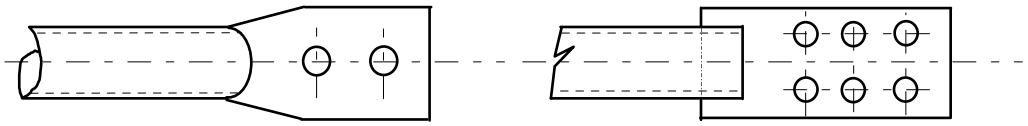

(a) flattened end detail (b) slotted end detail

Fig. 1 Type of end-connections

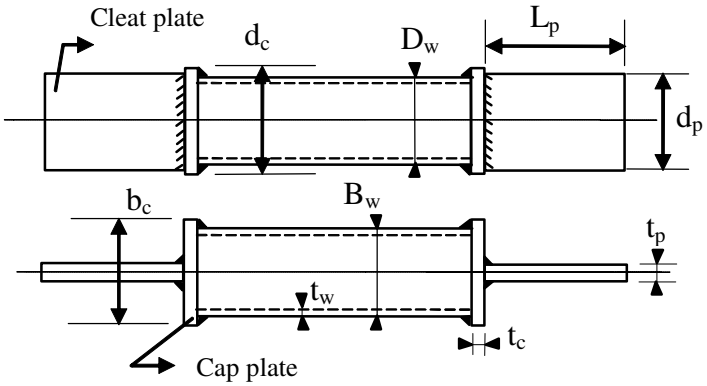

Fig. 2 Welded T-end connection and parameters definition

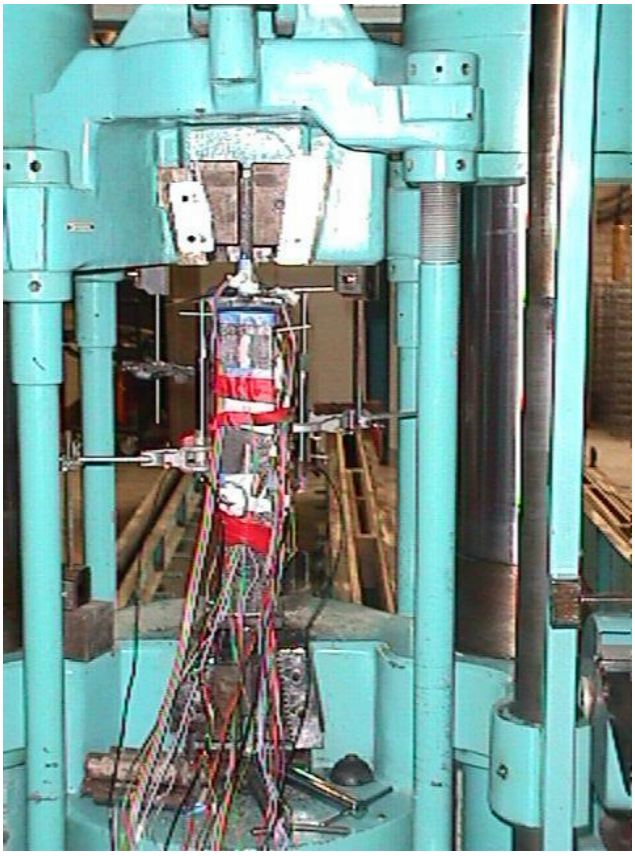

Fig. 3 Testing machine with specimen set-up

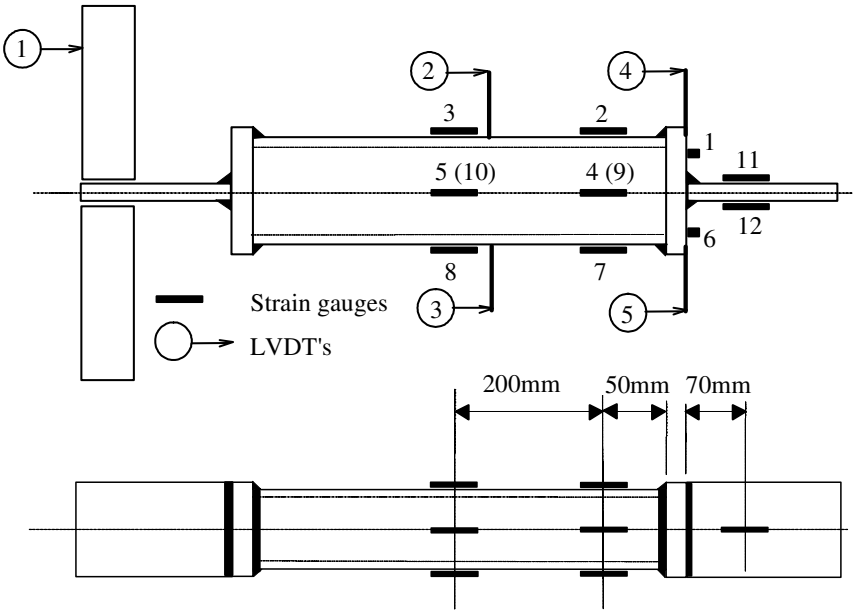

Fig. 4 Joint testing arrangements

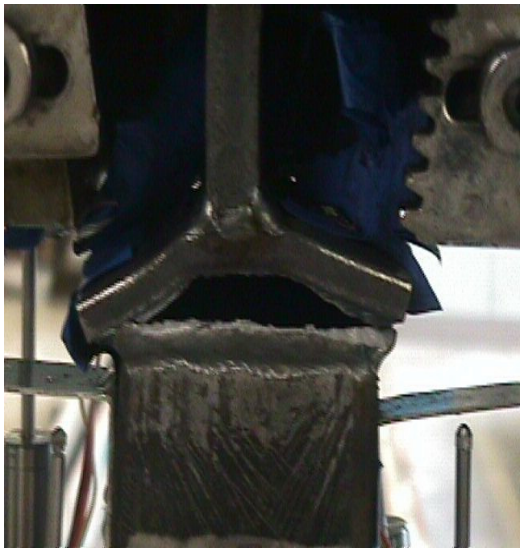

Fig. 5 Cap plate-to-tube weld fracture (Test 1, see Table 2)

Fig. 6 Typical tube yielding (Test 3, see Table 2)

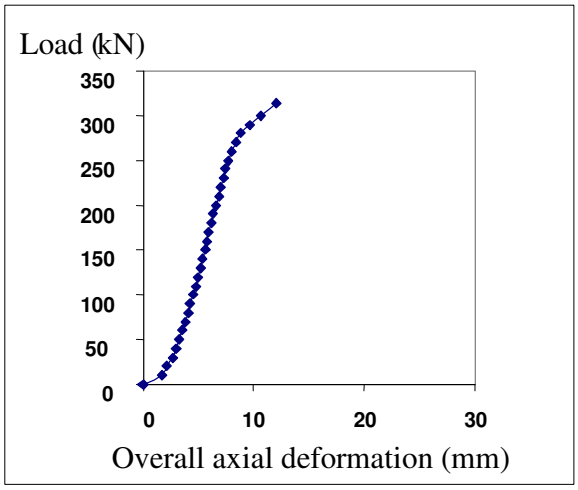

Fig. 7 Load vs axial deformation for specimen 8 (LVDT1, see Fig. 4)

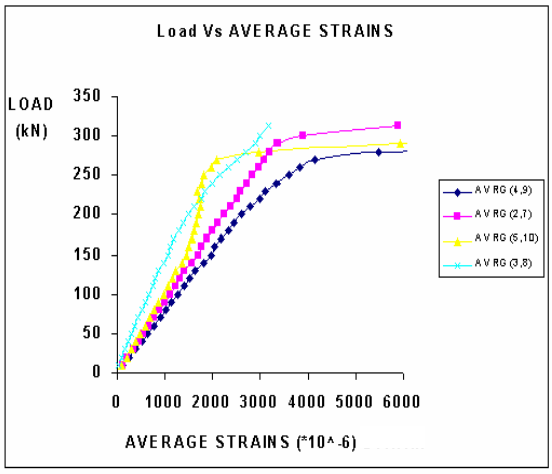

Fig. 8 Load vs averaged strains for specimen 8 (Read in conjunction with Figs. 3 and 4)

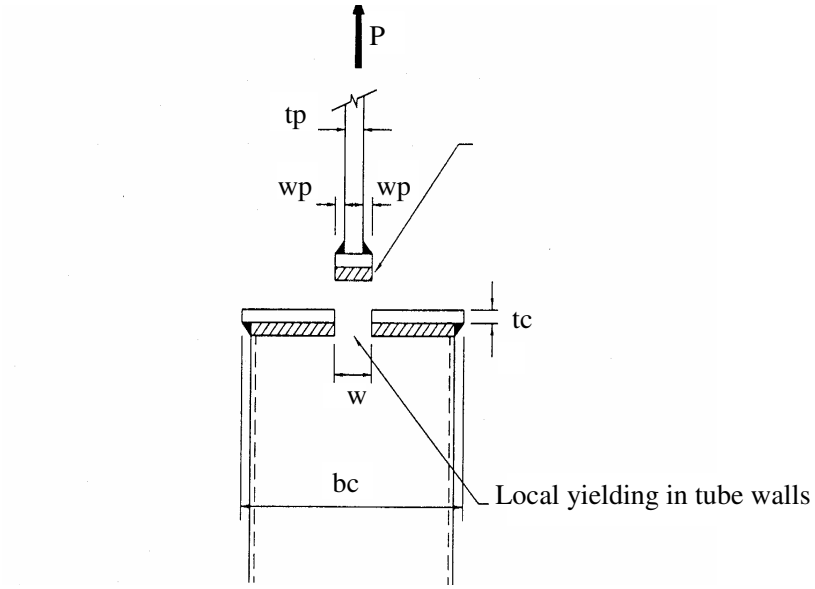

Fig. 9 Shearing failure of cap plate and parameters

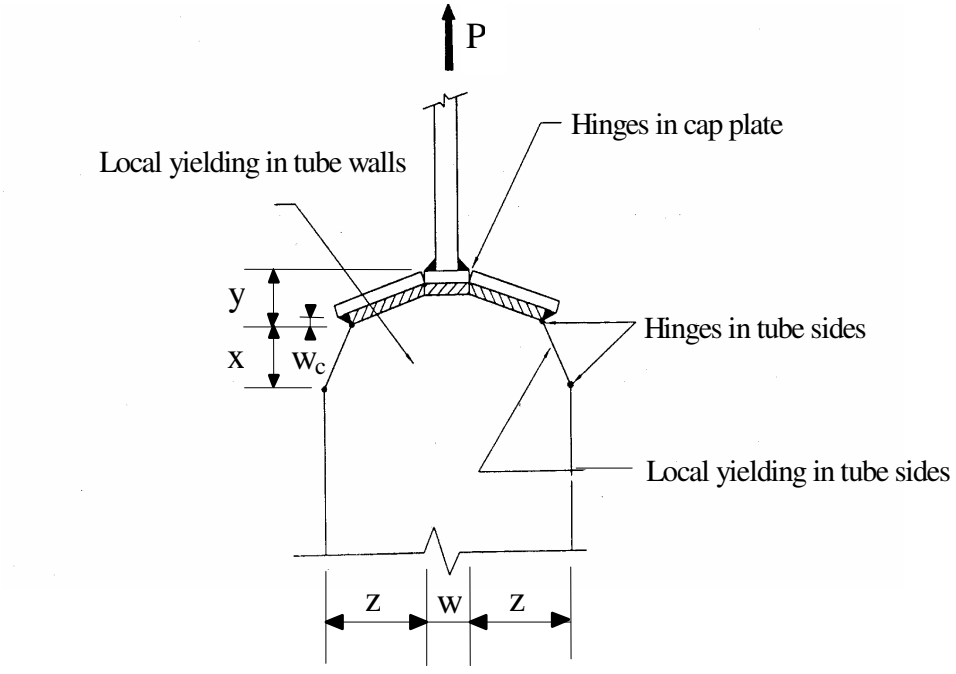

Fig. 10 Plastic hinges in cap plate and tube sides

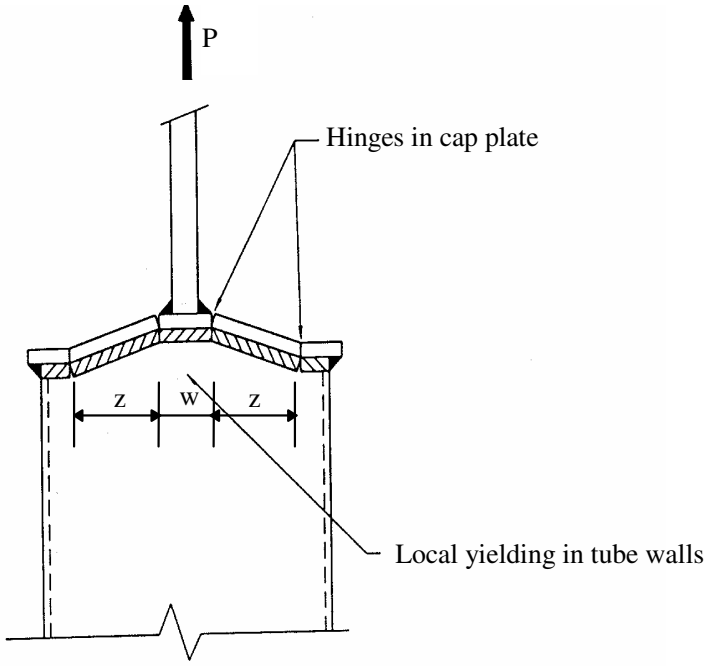

Fig. 11 Plastic hinges in cap plate

Table 1
Geometry of specimens

Test No.		Tube dimensions (mm)			Cap plate dimensions (mm)			Cleat plate dimensions (mm)	
		t_w	B_w	D_w	t_c	b_c	d_c	t_p	d_p
1		3.92	59.96	59.92	9.95	79.97	79.95	14.92	79.94
2		3.89	60.02	59.83	9.92	80.04	79.70	14.96	79.81
3		3.95	59.65	59.91	15.06	79.90	79.93	15.07	79.92
4		4.00	59.75	59.89	19.93	79.96	80.20	15.02	80.02
5		4.00	60.10	59.69	25.04	80.08	79.97	14.89	79.86
6		3.91	59.93	60.12	25.89	79.95	79.91	14.75	79.91
7		4.02	59.63	59.85	27.97	79.87	79.77	14.79	80.09
8		3.89	59.81	60.21	30.06	79.94	79.92	15.11	80.15
9		4.07	79.93	79.88	19.95	99.97	100.00	15.09	99.80
10		3.95	80.12	79.93	14.87	100.08	99.92	14.79	99.90
11		3.95	80.66	80.13	20.11	98.98	99.76	15.15	99.85
12	Cleat plate	3.97	59.91	39.94	9.98	79.98	58.87	14.83	78.91
13	parallel to	4.06	60.35	39.97	14.90	80.40	60.07	14.96	80.05
14	longer side	4.01	79.78	40.22	10.00	99.85	59.85	14.92	99.76
15	of tube	3.98	79.60	39.96	15.06	99.80	59.86	15.09	100.07
16	Cleat plate	3.87	39.50	59.87	9.97	59.63	79.63	15.12	59.92
17	parallel to	4.07	39.12	60.12	14.96	59.70	79.84	14.97	59.95
18	shorter side	3.92	39.72	79.86	10.04	59.87	79.90	15.00	59.86
19	of tube	3.89	39.90	80.21	14.97	59.98	100.02	14.91	60.12

Table 2
Summary of test results

Specimen	P_Y (kN) (yield strength)	P_{UE} (kN) (test failure load)	P_{UE}/P_Y	Failure mode
1	351	240	0.68	Weld Fracture
2	348	280	0.80	Tube yielding and hinges in cap plate
3	352	300	0.85	Tube yielding
4	357	320	0.90	Tube yielding
5	321	350	1.09	Tube yielding
6	315	330	1.05	Tube yielding
7	321	320	1.00	Tube yielding
8	313	310	0.99	Tube yielding
9	485	330	0.68	Local fracture
10	472	420	0.89	Tube yielding
11	474	450	0.95	Tube yielding
12	304	300	0.99	Local fracture
13	312	330	1.06	Tube yielding
14	339	240	0.71	Local Fracture
15	335	260	0.78	Tube yielding
16	265	280	1.06	Tube yielding
17	277	300	1.08	Tube yielding
18	347	230	0.66	Tube yielding
19	347	240	0.69	Tube yielding

Table 3
Failure loads: Test results versus yield line predictions

Specimen	P1	P2	P3	P4	P5	P_{UT} (kN) (Yield line)	P_{UE} (kN) (Tests)	P_{UE}/P_{UT}
1	351	435	392	424	409	351	240	0.68
2	348	436	391	421	408	348	280	0.80
3	352	440	538	626	760	352	300	0.85
4	357	439	678	887	1226	357	320	0.90
5	321	434	812	1191	1844	321	350	1.09
6	315	430	832	1210	1900	315	330	1.05
7	321	432	893	1401	2239	321	320	1.00
8	313	442	951	1551	2546	313	310	0.99
9	485	550	820	658	871	485	330	0.68
10	472	539	636	473	553	472	420	0.89
11	474	552	816	648	865	474	450	0.95
12	304	427	399	4891	5079	304	300	0.99
13	312	437	544	10039	13460	312	330	1.06
14	339	543	460	5056	5603	339	240	0.71
15	335	551	639	12702	18164	335	260	0.78
16	265	331	313	347	333	265	280	1.06
17	277	328	423	505	588	277	300	1.08
18	347	328	322	298	277	277	230	0.83
19	347	327	426	371	402	327	240	0.73